2004

P Pilus assembly motif necessary for activation of the CpxRA pathway by PapE in Escherichia coli

Yvonne M. Lee
Washington University School of Medicine in St. Louis

Patricia A. DiGiuseppe
Princeton University

Thomas J. Silhavy
Princeton University

Scott J. Hultgren
Washington University School of Medicine in St. Louis

Recommended Citation

Lee, Yvonne M.; DiGiuseppe, Patricia A.; Silhavy, Thomas J.; and Hultgren, Scott J., "P Pilus assembly motif necessary for activation of the CpxRA pathway by PapE in Escherichia coli." Journal of Bacteriology. 186, 13. 4326-4337. (2004).
https://digitalcommons.wustl.edu/open_access_pubs/2712

P Pilus Assembly Motif Necessary for Activation of the CpxRA Pathway by PapE in *Escherichia coli*

Yvonne M. Lee, Patricia A. DiGiuseppe, Thomas J. Silhavy and Scott J. Hultgren

J. Bacteriol. **2004, 186(13):4326. DOI: 10.1128/JB.186.13.4326-4337.2004.**

JOURNAL OF BACTERIOLOGY, July 2004, p. 4326–4337 Vol. 186, No. 13
0021-9193/04/$08.00+0 DOI: 10.1128/JB.186.13.4326–4337.2004

P Pilus Assembly Motif Necessary for Activation of the CpxRA Pathway by PapE in *Escherichia coli*

Yvonne M. Lee,[1] Patricia A. DiGiuseppe,[2] Thomas J. Silhavy,[2] and Scott J. Hultgren[1]*

Department of Molecular Microbiology, Washington University School of Medicine, St. Louis, Missouri 63110,[1] and Department of Molecular Biology, Princeton University, Princeton, New Jersey 08544[2]

Received 16 December 2003 /Accepted 29 March 2004

P pilus biogenesis occurs via the highly conserved chaperone-usher pathway, and assembly is monitored by the CpxRA two-component signal transduction pathway. Structural pilus subunits consist of an N-terminal extension followed by an incomplete immunoglobulin-like fold that is missing a C-terminal seventh beta strand. In the pilus fiber, the immunoglobulin-like fold of each pilin is completed by the N-terminal extension of its neighbor. Subunits that do not get incorporated into the pilus fiber are driven "OFF-pathway." In this study, we found that PapE was the only OFF-pathway nonadhesin P pilus subunit capable of activating Cpx. Manipulation of the PapE structure by removing, relocating within the protein, or swapping its N-terminal extension with that of other subunits altered the protein's self-associative and Cpx-activating properties. The self-association properties of the new subunits were dictated by the specific N-terminal extension provided and were consistent with the order of the subunits in the pilus fiber. However, these aggregation properties did not directly correlate with Cpx induction. Cpx activation instead correlated with the presence or absence of an N-terminal extension in the PapE pilin structure. Removal of the N-terminal extension of PapE was sufficient to abolish Cpx activation. Replacement of an N-terminal extension at either the amino or carboxyl terminus restored Cpx induction. Thus, the data presented in this study argue that PapE has features inherent in its structure or during its folding that act as specific inducers of Cpx signal transduction.

A critical factor in the establishment of pyelonephritis by uropathogenic *Escherichia coli* is the P pilus, which mediates bacterial attachment to the urinary tract (29, 40, 41, 49). P pili carry an adhesin, PapG, that binds to Galα(1-4)Gal-containing glycolipids on the surfaces of urothelial cells lining the human kidney (5, 22, 33, 34, 37, 58). The ability to adhere to specific receptors in the host tissue allows the pathogens to gain a foothold in the tissue and subsequently to cause disease (41, 49).

P pili consist of a thin tip fibrillum connected to a thicker cylindrical rod (30) (Fig. 1A). Their assembly requires the coordination of at least 11 structural and regulatory gene products encoded within the *pap* gene cluster (20, 36). The tip fibrillum is flexible and consists mainly of PapE subunits interacting linearly with each other to form an open helical configuration, approximately 2 to 3 nm in diameter (30). The PapG adhesin localizes to the distal tip of the fibrillum (30, 34) and is believed to be joined to the rest of the structure through the adaptor protein PapF (27). The more rigid pilus rod contains PapA subunits arranged to form a right-handed helical cylinder (2) with 3.28 subunits per turn (6, 17). The tip fibrillum portion of the pilus is connected to the rod via the PapK adaptor (27). PapH is thought to anchor the entire composite pilus structure to the bacterial envelope (1).

As with any multimeric structure, assembly is an intricate process. P pili are assembled through the highly conserved chaperone-usher pathway (19, 59, 60). This pathway is also used to build hundreds of other adhesive organelles in various gram-negative organisms (references 21 and 24 and unpublished data). In P pilus biogenesis, subunits are translocated into the periplasm via the general protein export (*sec*) machinery, where they interact with the chaperone, PapD (59, 60). This interaction facilitates subunit folding (3, 50). Folded subunits remain bound to the chaperone, which serves to stabilize the subunits and prevent them from undergoing nonproductive interactions that would lead to their aggregation and eventual degradation (3, 26, 28, 31, 51). Chaperone-subunit complexes are targeted to the PapC usher assembly site (31, 35, 54, 57, 62). The PapC usher is a multimeric structure arranged as a 2- to 3-nm channel that differentially binds the various chaperone-subunit complexes (15, 53, 61). At the usher, the chaperone is dissociated from the pilus subunit (23), exposing the subunit's underlying interactive surfaces, and driving assembly across the outer membrane into the final pilus fiber (23, 52, 53, 61).

The three-dimensional structures of PapD-PapK and PapD-PapE chaperone-subunit complexes showed that pilus subunits have an incomplete immunoglobulin-like (Ig-like) fold in that they are missing a C-terminal seventh beta strand (50, 51). The absence of this C-terminal beta strand results in exposure of a large hydrophobic groove in the subunits (50, 51). Pilus subunits also contain an amino-terminal (N-terminal) extension preceding the first A1 beta strand (50, 51). The N-terminal extensions of P pilus subunits vary in length but all contain a conserved motif of alternating hydrophobic residues (50, 51, 56). All pilus subunits are expected to have the same topology (8, 50, 51, 56). Chaperones consist of two complete Ig-like domains oriented such that they form an overall boomerang-like conformation (8, 18, 23–25, 32, 50). The chaperone functions by donating its G1 beta strand to complete the Ig-like

* Corresponding author. Mailing address: Department of Molecular Microbiology, Washington University School of Medicine, 660 South Euclid Ave., Campus Box 8230, St. Louis, MO 63110. Phone: (314) 362-6772. Fax: (314) 362-1998. E-mail: hultgren@borcim.wustl.edu.

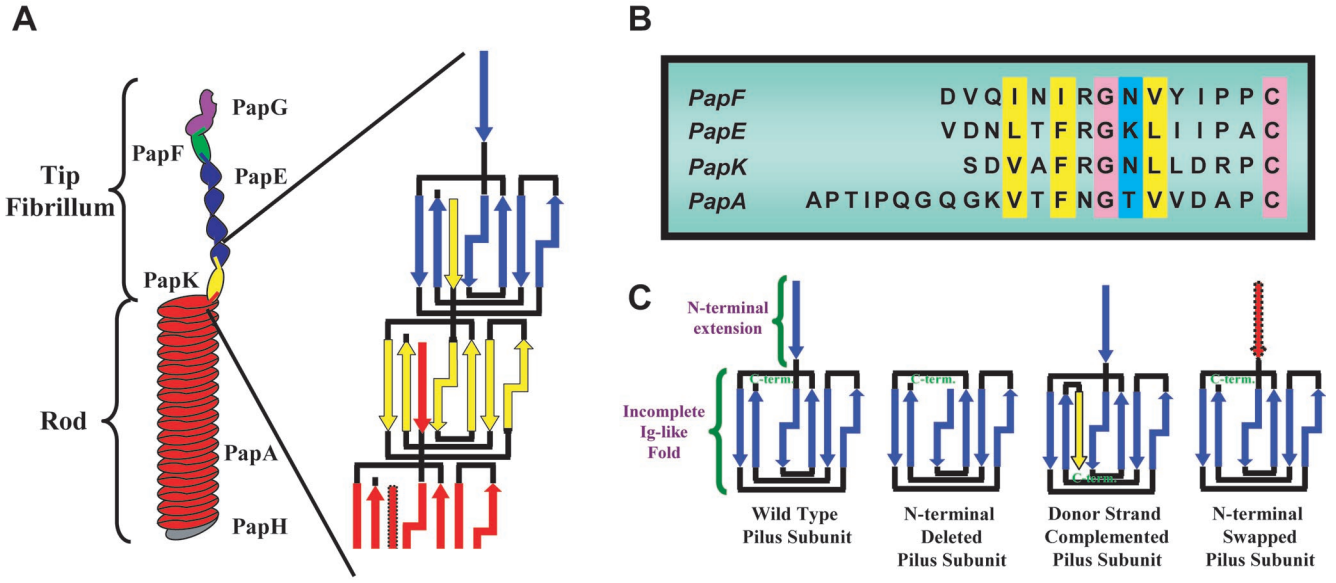

FIG. 1. Structural subunits forming the pilus consist of an Ig-like fold and an amino-terminal extension. (A) Schematic diagram of a P pilus fiber. Structural proteins making up the pilus fiber are arranged in a specific order to form the final pilus structure. The tip fibrillum consists of the PapG adhesin (purple) at the distal end followed by the PapF adaptor protein (green). PapE (blue) self-associates into a linear open helical polymer. The tip fibrillum is attached to the PapA (red) rod via the adaptor protein PapK (yellow). The whole pilus fiber is anchored to the bacterial cell membrane by PapH (grey). Subunits interact with each other via donor strand exchange, schematically shown for PapE, PapK, and PapA. (B) Amino-terminal extension alignment of P pilus subunits. The sequences of the amino termini of nonadhesin P pilus subunits exhibit two invariant residues (pink columns) and a conserved motif of alternating hydrophobic residues (yellow columns) within the N-terminal extension. However, each N-terminal extension is unique to a particular pilus protein, and the region varies in length among the subunits. (C) Schematic diagram of mutants used in this work. Wild-type pilus subunits consist of an incomplete Ig-like fold preceded by an amino-terminal extension. In N-terminal deleted subunits, the N-terminal extension was removed. In donor strand complemented subunits, a DNKQ loop followed by a donor strand (yellow) was genetically fused to the carboxyl end of the subunit. The N-terminal extension of one subunit was "swapped" with the same region of another subunit (red strand) in N-terminal swapped mutants.

fold of the subunit by inserting parallel to the F beta strand of the pilin in a process called donor strand complementation (8, 50).

Pilus assembly occurs via donor strand exchange, in which occupation of a pilin subunit groove by the chaperone is exchanged for an N-terminal extension from an incoming preassembled subunit (3, 8, 50, 51). In contrast to donor strand complementation, the N-terminal extension of a subunit inserts antiparallel to the C-terminal F beta strand of its neighboring subunit, creating a stable canonical Ig-like fold (3, 8, 50, 51). The basis by which specificity in the donor strand exchange process defines the order of subunit incorporation into a pilus fiber has not been demonstrated.

In the absence of the chaperone, P pilus subunits are diverted "OFF-pathway," causing them to participate in nonproductive interactions (26, 28). During normal pilus assembly, a portion of pilus subunits fail to interact with the chaperone and are consequently not incorporated into a growing pilus (26, 28). They, too, are driven OFF-pathway (26, 28). Two of these subunits have been shown to activate partially overlapping stress responses: the PapG adhesin activates the CpxRA and BaeSR two-component signal transduction pathways, as well as the alternate sigma factor σ^E pathway, whereas PapE activates the CpxRA pathway and may also activate the BaeSR pathway (14, 26, 28, 44, 47). Both the Cpx and σ^E pathways are finely tuned to respond to extracytoplasmic stresses (9, 10, 12, 46, 47), and each regulates the expression of genes encoding periplasmic protein folding factors and proteases that alleviate periplasmic and membrane disruptions (9, 10, 12, 46, 47). Furthermore, an expanded repertoire of potential Cpx-regulated genes has recently been reported (13), and predicted Cpx binding sites have been found upstream of virulence factors such as hemolysin, P pili, type 1 pili, and cytotoxic necrotizing factor 1, suggesting that this pathway may also play a significant role in pathogenesis (26).

The CpxRA two-component signaling pathway consists of the sensor histidine kinase CpxA in the inner membrane and the response regulator CpxR in the cytoplasm (9, 10, 12, 46, 47). CpxA has been shown to have three activities: autokinase, CpxR kinase, and CpxR phosphatase (48). The phosphorylation of CpxR, which is thought to occur in response to stress (47), increases its binding affinity for specific recognition motifs upstream of target genes in vitro (43, 47, 48). Negative autoregulation of the pathway is accomplished through CpxP (45, 46, 48). CpxP is a periplasmic protein, itself regulated by Cpx (11, 45, 46), that leads to down-regulation of the system in a CpxA-dependent manner (45, 46). Stresses that activate the pathway inactivate CpxP (14). The pathway responds to diverse stresses, including overproduction of the lipoprotein NlpE (55), alkaline pH (42), changes in lipid composition in the inner membrane (38), and certain OFF-pathway pilus subunits (28). It is currently thought that these stresses may ulti-

TABLE 1. Strains and plasmids used in this work

Strain or plasmid	Description	Reference
Strains		
MC4100	F$^-$ *araD139* Δ*(argF-lac)U169 rpsL150* (Str^r) *relA1 flbB5301 deoC1 ptsF25 rbsR*	7
TR50	MC4100 λRS88 [*cpxP′-lacZ*$^+$]	48
MC1061	F$^-$ *araD139* Δ*(ara-leu)7696 galE15 galK16* Δ*(lac)X74 rpsL* (Str^r) *hsdR2*(r_K^- m_K^+) *mcrA mcrB1*	63
Plasmids		
pMMB66	Expression vector	16
pPAP5	Wild-type *pap* operon	36
pWT	PapD expression plasmid	23
pTRC-G1	*papG1*	K. Dodson, unpublished data
pFJ7	*papF*	27
pHJ13	Wild-type PapE expression plasmid	28
pFJ11	*papK*	27
pFGS2	N-terminally deleted *papE*	51
pYML33	Dsc_EPapE expression plasmid	This study
pYML34	Dsc_KPapE expression plasmid	This study
pYML36	NtdPapE expression plasmid	This study
pYML42	Wild-type PapG1 expression plasmid	This study
pYML43	Wild-type PapF expression plasmid	This study
pYML44	Wild-type PapK expression plasmid	This study
pYML50	Wild-type PapA expression plasmid	This study
pYML55	Nts_EPapF expression plasmid	This study
pYML56	Nts_FPapE expression plasmid	This study
pYML64	NtdPapF expression plasmid	This study
pYML75	Nts_EPapK expression plasmid	This study
pYML80	Nts_EPapA expression plasmid	This study
pYML83	Nts_KPapE expression plasmid	This study
pYML87	Nts_APapE expression plasmid	This study

mately lead to misfolded proteins in the cell envelope, which are then sensed by the Cpx pathway (14); however, the precise details of Cpx activation remain unclear.

In this study, we found that PapE was the only nonadhesin P pilus subunit capable of activating the Cpx pathway. Surprisingly, even though PapA is the most abundantly expressed subunit and is highly aggregative, it did not induce Cpx. We therefore investigated the structural basis by which PapE specifically activates Cpx. We constructed a series of N-terminal deleted, donor strand complemented, and N-terminal swapped pilin subunits and characterized their abilities to participate in subunit-subunit interactions and Cpx activation. We discovered that deletion of the N-terminal extension from PapE abolished its ability to induce Cpx. We also demonstrated that the N-terminal extension influences the proper association between subunits in the pilus, conferring specificity in subunit-subunit interactions consistent with the donor strand exchange hypothesis. In conclusion, subunit aggregation and stability in the periplasm did not correlate with Cpx induction. Instead, induction was related to structural features of PapE.

MATERIALS AND METHODS

Bacterial strains and genetic constructs. All bacterial strains and constructs are listed in Table 1. The *E. coli* K-12 strain MC4100 (7) was used as the host strain in all studies, except in cloning steps. Plasmids were constructed in the *E. coli* K-12 strain MC1061 (63). TR50 (MC4100 λRS88[*cpxP′-lacZ*$^+$]) has been previously characterized (48).

The vector pMMB66 (16) was used to express pilus subunits under the control of the P_{tac} promoter. pMMB66 was digested with the same restriction enzymes used to generate the inserts as described below. pYML36 contains NtdPapE from the EcoRI-BamHI fragment of pFGS2 (51). pYML42 contains *papGI* from the EcoRI-BamHI fragment of pTRC-G1 (kind gift of Karen Dodson, Washington University). pYML43 contains *papF* from the EcoRI-SalI fragment of pFJ7 (27). pYML44 contains *papK* from the EcoRI-SalI fragment of pFJ11 (27).

pYML33 contains Dsc_EPapE under the control of P_{tac}. Dsc_EPapE was amplified by PCR from pPAP5 (36) while adding a donor strand to the 3′ end of the gene as well as EcoRI and BamHI sites on the 5′ and 3′ ends, respectively. The oligonucleotides (primers are labeled a to y in this section) used in this process were a (5′-ACAGTGGAATTCGTGATGAAAAAGATAAGAGGTTTGTGTC-3′) and b (5′-CGCGGATCCTTAGGCAGGAATAATCAGTTTTCCTCTGAAGGTCAGATTATCAACTTGTTTGTTATCCGAATATGATGCAACCAGCGTTGCTGTTGCAGAG-3′). pYML34 contains Dsc_KPapE and was amplified in the same manner, with oligonucleotides a (from above) and c (5′-CGCGGATCCTTAGGGTCTGTCAAGCAGATTACCCCTGAATGCCACATCTGATTGTTTGTTATCCGAATATGATGCAACCAGCGTTGCTGTTGCAGAGAA-3′). pYML50 contains wild-type *papA* amplified from pPAP5 without any modification except to add EcoRI and BamHI restriction enzyme sites to the 5′ and 3′ ends of the gene, respectively. The oligonucleotides used in this procedure were d (5′-CCGGAATTCTGCCAGATATCTCTGGTG-3′) and e (5′-CGCGGATCCGATAAATACCCTGAG-3′).

Other mutagenesis was performed by using a two-step PCR technique described previously (39). The plasmid pYML55, containing Nts_EPapF, was constructed by using the following oligonucleotides (f through i) to (i) replace the DNA sequence corresponding to the 14-amino-acid N-terminal extension of PapF with the DNA sequence corresponding to the 14-amino-acid N-terminal extension of PapE and (ii) introduce EcoRI and BamHI sites to the 5′ and 3′ ends of the mutant gene, respectively: f, 5′-CCGGAATTCTTTCTGTACCGCTCTCCG-3′; g, 5′-CGCGGATCCCACTTCCGTAATTACAGT-3′; h, 5′-TCGGTCGCTGTACTGGCTGTTGATAATCTGACCTTCAGAGGAAAACTGATTATTCCTGCCTGCACCATTAATAACGGG-3′; i, 5′-CCCGTTATTAATGGTGCAGGCAGGAATAATCAGTTTTCCTCTGAAGGTCAGATTATCAACAGCCAGTACAGCGACCGA-3′. pYML56, to express the mutant Nts_FPapE, was constructed in the same way as pYML55 by using the following oligonucleotides: j, 5′-CCGGAATTCATGAAAAAGATAAGAGGT-3′; k, 5′-CGCGGATCCGGAGAGCGGTACAGA-3′; l, 5′-ATGTCTCAGCATGTACATGCAGATGTGCAGATTAACATCAGGGGGAATGTTTATATCCCCCCATGTACTGTAAGCAACACAACTG-3′; m, 5′-CAGTTGTGTTGCTTACAGTACATGGGGGGATATAAA

CATTCCCCCTGATGTTAATCTGCACATCTGCATGTACATGCTGAGACA T-3′. To construct the plasmid pYML64, which contains NtdPapF, oligonucleotides f and g, described above, were used in addition to the following primers to delete the DNA sequence encoding residues 2 to 12 of the N-terminal extension of PapF and to introduce EcoRI and BamHI sites to the 5′ and 3′ ends of the mutant gene, respectively: n, 5′-TCGGTCGCTGTACTGGCTGATCCCCCATGCACCATTAA TAAC-3′; o, 5′-GTTATTAATGGTGCATGGGGGATCAGCCAGTACAGCGA CCGA-3′. The plasmid pYML75, which contains Nts_EPapK, was made similarly to pYML55 and pYML56, with the following oligonucleotides, to replace the 13-amino-acid N-terminal extension of PapK with the 14-amino-acid N-terminal extension of PapE: p, 5′-CCGGAATTCGGGAATGTGATGATAAAAAGCA CAGGC-3′; q, 5′-CGCGGATCCCTGAAATATCCTGTACAA-3′; r, 5′-CTGC CGGACAGGCAATAGCCGTTGATAATCTGACCTTCAGAGGAAAACTG ATTATTCCTGCCTGCCATGTGTCCGGTGAC-3′; s, 5′-GTCACCGGACA CATGGCAGGCAGGAATAATCAGTTTTCCTCTGAAGGTCAGATTATC AACGGCTATTGCCTGTCCGGCAG-3′. The plasmid pYML80, containing Nts_EPapA, was constructed by using oligonucleotides d and e from above with the following oligonucleotides: t, 5′-GTGGTGTCTTTTGGTGTAAATAATGCT GTTGATAATCTGACCTTCAGAGGAAAACTGATTATTCCTGCCTGCAGC ATTTCTCAGAAATCAGCTG-3′; u, 5′-CAGCTGATTTCTGAGAAATGCTGC AGGCAGGAATAATCAGTTTTCCTCTGAAGGTCAGATTATCAACAGC ATTATTTACACCAAAAGACACCAC-3′. The plasmid pYML83, containing Nts_KPapE, was also made similarly to the others, by using primers j and k from above together with the following oligonucleotides: v, 5′-ATGTCTCAGCATG TACATGCATCAGATGTGGCATTCAGGGGTAATCTGCTTGACAGACC CTGTACTGTAAGCAACACAACTG-3′; w, 5′-CAGTTGTGTTGCTTACAG TACAGGGTCTGTCAAGCAGATTACCCCTGAATGCCACATCTGATGC ATGTACATGCTGAGACAT-3′. The plasmid pYML87, containing Nts_APapE, was made with primers j and k from above and the following primers: x, 5′-TC TCAGCATGTACATGCAGCTCCAACTATTCCACAGGGGCAGGGTAAA GTAACTTTTAACGGAACTGTTGTTGATGCTCCATGTACTGTAAGCAA CACAA-3′; y, 5′-TTGTGTTGCTTACAGTACATGGAGCATCAACAACAG TTCCGTTAAAAGTTACTTTACCCTGCCCCTGTGGAATAGTTGGAGCT GCATGTACATGCTGAGA-3′. Amplified PCR inserts were cloned using a TOPO-TA kit (Invitrogen), and mutations were confirmed by sequencing. The fragments were then digested with EcoRI and BamHI and subcloned into pMMB66.

The following plasmids have been previously described elsewhere. The plasmid pPAP5 encodes the entire wild-type *pap* operon under control of the native promoter (36). pHJ13 contains wild-type *papE* under the control of the P_{tac} promoter in pMMB66 (28). pWT contains *papD* under the control of a P_{ara} promoter (23).

β-Galactosidase assays. Saturated bacterial cultures were diluted 1:100 in Luria-Bertani (LB) broth and grown in the presence of appropriate antibiotics to mid-logarithmic phase (optical density at 600 nm, ~0.5 to 0.6). Isopropyl-β-D-thiogalactopyranoside (IPTG) was added to 0.1 mM for induction from P_{tac}. The cells were then allowed to continue to grow, and 1-ml samples were taken at various time points over a 4-h time course for the β-galactosidase assay. β-Galactosidase assays were performed on these samples as previously described (26). β-Galactosidase activity for all assays is reported in this study at the 180-min time point following induction by IPTG (the time point chosen represents the average point of peak Cpx activation by PapE).

To compare Cpx activation and pilus subunit stability in the periplasm, cells were grown and induced as described above. At 180 min postinduction (same time point reported in assays above), β-galactosidase assays were performed as described, and then remaining cells were harvested and periplasms were isolated as described below.

Periplasmic extract preparations. Bacterial cells grown to saturation in 10 ml of LB broth supplemented with 0.8% glucose and appropriate antibiotics were harvested by centrifugation and resuspended in 10 ml of fresh LB broth twice. Cells were diluted 1:40 in LB broth and grown in the presence of appropriate antibiotics. When preparing periplasms from strains carrying a plasmid to produce a pilus subunit or a mutant subunit from a P_{tac} promoter, IPTG was added to 0.1 mM to cells grown to logarithmic phase. In strains containing pWT, PapD was induced with arabinose to 0.1%. Growth was then allowed to continue for 90 min before the preparation of periplasmic extracts. Periplasms were isolated by the sucrose-lysozyme method as described previously (15).

Sodium dodecyl sulfate (SDS) sample buffer was added to each extract, and samples were incubated for 5 to 10 min at 95°C. Periplasmic extracts were analyzed by SDS-polyacrylamide gel electrophoresis (PAGE) followed by immunoblotting with rabbit antisera raised against Pap pilus tip fibrillae (reactive against PapG, PapF, PapE, and PapK) as the primary antibody and alkaline phosphatase-conjugated goat anti-rabbit IgG (Sigma) as the secondary antibody.

Self-association assays. Periplasmic extracts were prepared as described above and treated with SDS sample buffer. Each sample was incubated for 5 to 10 min at either 95 or 22°C (room temperature). Samples were then analyzed by SDS-PAGE followed by staining with Coomassie blue, as well as by Western blotting. Immunoblotting was done by using Pap pilus tip antiserum as described above.

RESULTS

Mutagenesis strategy. The assembly of pili requires that pilus subunits interact with the PapD chaperone (3, 26, 28, 31, 51). PapE subunits that fail to interact with PapD fall OFF-pathway and activate the Cpx pathway, resulting in their nonproductive aggregation and eventual degradation (28). The crystallization of PapE was impeded by these aggregation problems; however, Sauer et al. showed that the nonproductive aggregation could be eliminated by removal of the N-terminal extension, creating N-terminal deleted PapE (51). The N-terminal extension is comprised of a highly conserved motif consisting of alternating hydrophobic residues (Fig. 1B) (50, 51, 56). A conserved cysteine demarcates the end of this region and the subsequent beginning of the first A1 beta strand of the Ig-like fold (50, 51). In addition to these similarities, the N-terminal extensions also exhibit variations in length, and each consists of subunit-specific residues (Fig. 1B).

We created a series of "N-terminal deleted" (Ntd), "donor strand complemented" (Dsc), and "N-terminal swapped" (Nts) subunits (Fig. 1C). In N-terminal deleted subunits, NtdPapE (previously described) (51) and NtdPapF, residues 2 through 12 at the amino termini of the mature pilus subunits were deleted, resulting in proteins that lacked the amino-terminal extension, but retained their signal sequences and incomplete Ig-like folds (Fig. 1C). Donor strand complemented proteins Dsc_EPapE and Dsc_KPapE were engineered as previously described for other pilus subunits (3). In a donor strand complemented subunit, fusion of a seventh beta strand to the C terminus completes its Ig-like fold, resulting in a subunit that is stable in the absence of the chaperone (3, 4). Dsc_EPapE was created by adding the first 14 amino acids (VDNLTFRG KLIIPA) of PapE to the C-terminal end of PapE, following a short DNKQ linker loop. Dsc_KPapE was constructed in the same way, with the first 13 amino acids (SDVAFRGNLLDRP) of PapK. We also created N-terminal swapped subunits, exchanging the complete N-terminal extension of one subunit with that of another (Fig. 1C). The first 14 amino acids of PapE were removed from the Ig-like domain of PapE and replaced with the first 14 residues (DVQINIRGNVYIPP) of PapF to produce Nts_FPapE. In a similar manner, the subunits Nts_KPapE and Nts_APapE were likewise generated. The N-terminal extensions of PapF, PapK, and PapA were also replaced with the N-terminal extension of PapE, making Nts_EPapF, Nts_EPapK, and Nts_EPapA, respectively. These N-terminal swapped subunits allow examination of the N-terminal extension as a whole unit, without disrupting the Ig-like domain of the pilus subunit. The chaperone PapD completes the fold of a subunit by providing the missing seventh beta strand in the Ig-like domain of the subunit; in the absence of this interaction, pilin subunits are unstable (3, 50). The stability of each of the mutants in the periplasm was therefore examined when coexpressed with the chaperone in the *E. coli* laboratory strain MC4100, which lacks the *pap* operon. All wild-type and N-terminal deleted and N-terminal swapped subunits

were stable in the periplasm when coexpressed with the chaperone (data not shown). Donor strand complemented subunits were stable in the periplasm with or without coexpression of the chaperone (data not shown).

The Cpx pathway discriminates between pilus subunits. Jones et al. discovered that pilus subunits that do not form complexes with the chaperone go OFF-pathway and may activate the Cpx pathway (28). Both PapG and PapE were shown to effectively induce the Cpx pathway when expressed in the absence of the chaperone (28). To understand the molecular basis for the Cpx response to OFF-pathway subunits, the ability of each of the other structural pilus subunits to activate the Cpx pathway in the absence of the chaperone PapD was tested. Cpx induction was measured by using β-galactosidase assays with the *E. coli* strain TR50, in which a *cpxP′-lacZ*$^+$ promoter fusion was integrated into the chromosome of MC4100 at the λ attachment site (11, 48). In these assays, growth of each culture was monitored by measuring absorbances at 600 nm, and Miller units take into account optical densities to allow for the direct comparison of β-galactosidase activities between samples. We discovered that the Cpx pathway is capable of discriminating between various pilus subunits. As shown previously, we found that production of PapG or PapE in the absence of PapD significantly induces the Cpx pathway (28) (Fig. 2A, compare first, second, and fourth bars). In contrast, PapF, PapK, and PapA were unable to activate the pathway (Fig. 2A, third, fifth, and sixth bars).

One explanation for the differential activation of Cpx by PapG and PapE, but not by PapF, PapK, and PapA, is that PapG and PapE may each be able to accumulate to higher levels than the other subunits in the periplasm in the absence of the chaperone. To examine this possibility, periplasmic extracts from cells producing each of the pilus subunits in the absence of PapD were analyzed by immunoblot analysis with antisera raised against P pili (recognizes PapA) and P tip fibrillae (recognizes PapG, PapF, PapE, and PapK) (Fig. 2B). All of the periplasms were prepared from cultures that were also used to assay β-galactosidase levels. These experiments revealed that only PapA was detectable in abundance under these conditions (Fig. 2B, lane 6). In contrast, PapE, the only pilin subunit capable of inducing Cpx, was undetectable in periplasmic extracts in the absence of PapD under these assay conditions (Fig. 2B, lane 4). Likewise, the other subunits, PapG, PapF, and PapK, were also not detected in the periplasmic extracts in the absence of PapD (Fig. 2B, lanes 2, 3, and 5, respectively). Thus, the differential recognition of PapE by the Cpx pathway cannot be explained simply by the levels of subunit accumulation in the periplasm in the absence of the chaperone. Instead, these results suggest that the Cpx pathway can distinguish between similar OFF-pathway subunits in the periplasm.

N-terminal extension is required for Cpx activation through PapE. Because PapE is the only nonadhesin pilus subunit capable of activating the Cpx pathway, we reasoned that PapE may be presenting a specific activating signal inherent in its structure to the Cpx pathway in the absence of PapD, either during or after its folding. The three-dimensional X-ray crystallographic structure of PapE has been previously solved and revealed that it consists of an N-terminal extension and an incomplete Ig-like fold (51). To investigate the contribution of each of these domains to the ability of PapE to activate the Cpx pathway, we compared the ability of wild-type PapE and NtdPapE to activate the Cpx pathway by analyzing the expression of *cpxP′-lacZ*$^+$ in strains producing either wild-type PapE or NtdPapE in the absence of the PapD chaperone (Fig. 3A). NtdPapE consists of the incomplete Ig-like pilin domain, con-

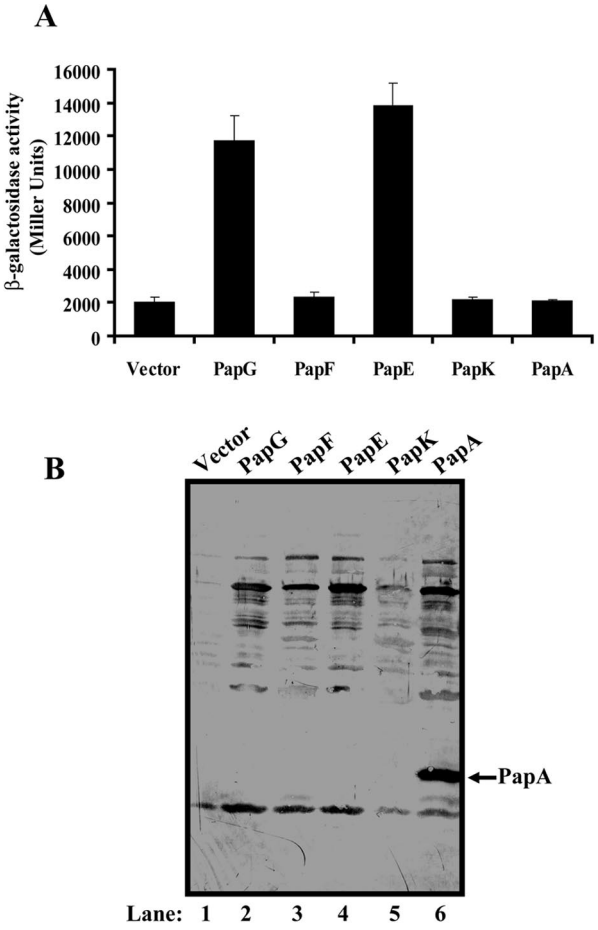

FIG. 2. Activation of the Cpx signaling pathway by P pilus structural proteins is restricted to PapE and PapG. (A) Cpx is differentially activated by P pilus subunits. Expression of a *cpxP′-lacZ*$^+$ fusion was analyzed. β-Galactosidase activity levels were assayed and are shown 180 min after induction of pilus subunits. This time point was selected because it corresponds to the average point of peak activation of the Cpx pathway by PapE. β-Galactosidase activity for the following strains is represented in Miller units, which take into account optical densities of the cultures assayed, enabling comparisons between samples: first bar, empty vector (TR50/pMMB66); second bar, PapG (TR50/pYML42); third bar, PapF (TR50/pYML43); fourth bar, PapE (TR50/pHJ13); fifth bar, PapK (TR50/pYML44); sixth bar, PapA (TR50/pYML50). The results plotted on the graph represent the means and standard deviations of the results from three assays. (B) Pilus subunit periplasm levels do not correlate to ability to activate Cpx. Pilus subunits in periplasms extracted following β-galactosidase assays from the following strains were visualized by immunoblot analysis developed with antiserum raised against P tip fibrillae (includes reactivity against PapG, PapF, PapE, and PapK) and antiserum raised against P pili (reactive against PapA): lane 1, empty vector control (TR50/pMMB66); lane 2, PapG (TR50/pYML42); lane 3, PapF (TR50/pYML43); lane 4, PapE (TR50/pHJ13); lane 5, PapK (TR50/pYML44); lane 6, PapA (TR50/pYML50). The subunit that was overexpressed is indicated above each lane of the immunoblot.

taining the hydrophobic groove due to the missing C-terminal beta strand, but has its N-terminal extension removed (51). Wild-type PapE subunits retain both the incomplete Ig-like fold and the N-terminal extension. As shown in Fig. 3A, PapE stimulated *cpxP′-lacZ*$^+$ transcription approximately sixfold over the vector control (compare first and second bars). In contrast, NtdPapE expression resulted in little or no activation of the Cpx pathway over the vector baseline (Fig. 3A, compare first and third bars). These results showed that deletion of the N-terminal extension of PapE abolished its ability to activate the Cpx pathway.

The inability of NtdPapE to activate Cpx suggested that the N-terminal extension was necessary for PapE to stimulate the Cpx pathway effectively. We hypothesized that the PapE N-terminal extension may also be sufficient for dictating PapE's ability to activate the Cpx pathway. To test the involvement of the specific PapE N-terminal extension in Cpx activation by PapE, *cpxP′-lacZ*$^+$ expression in response to production of Nts_EPapN subunits (where N is a non-PapE pilin subunit) in the absence of the chaperone was next analyzed by β-galactosidase assays (Fig. 3B). We found that expression of Nts_EPapF, which differs from wild-type PapF only in that it contains the N-terminal extension of PapE, did not stimulate *cpxP′-lacZ*$^+$ transcription to levels above those of the vector control (Fig. 3B, compare first and second bars). Similar to Nts_EPapF, Nts_EPapK also did not significantly activate the Cpx pathway (Fig. 3B, third bar). Interestingly, deletion of the N-terminal extension of PapA (NtdPapA) also converted it to a Cpx inducer (~3- to 4-fold) (data not shown). Thus, not surprisingly, the subunit Nts_EPapA was also able to activate the Cpx pathway, exhibiting approximately fourfold induction over the baseline set by the vector control (Fig. 3B, compare first and fourth bars). In this case, Cpx activation is presumably the result of the disruption of PapA rather than the presence of the PapE N-terminal extension. Overall, these Nts_EPapN results suggest that the N-terminal extension, though required, is not sufficient for activation of Cpx in response to the overproduction of PapE.

The studies described above demonstrated that, when expressed alone, the PapE Ig-like domain (NtdPapE) is incapable of activating the Cpx pathway; however, the N-terminal extension of PapE is not sufficient for recognition of PapE by the Cpx pathway. We hypothesized that the Ig-like fold of PapE may also contain information necessary for stimulation of the Cpx pathway when expressed in the context of its N-terminal extension. To investigate whether the wild-type N-terminal extension of PapE was specific for creating the signal or whether other N-terminal extensions could substitute for the wild-type PapE sequence when connected to the PapE Ig-like fold, levels of *cpxP′-lacZ*$^+$ transcription following expression of Nts_FPapE, Nts_KPapE, and Nts_APapE were measured (Fig. 3C). All of these subunits contain an intact PapE incomplete Ig-like domain, but each carries a different N-terminal extension. All Nts_NPapE subunits were able to activate the Cpx pathway in the absence of the PapD chaperone (Fig. 3C), though to significantly lower extents than wild-type PapE. Nts_FPapE produced an ~2-fold induction over the vector baseline control (Fig. 3C, compare first and second bars). Nts_KPapE and Nts_APapE activated Cpx to approximately threefold over the vector control (Fig. 3C, third and fourth

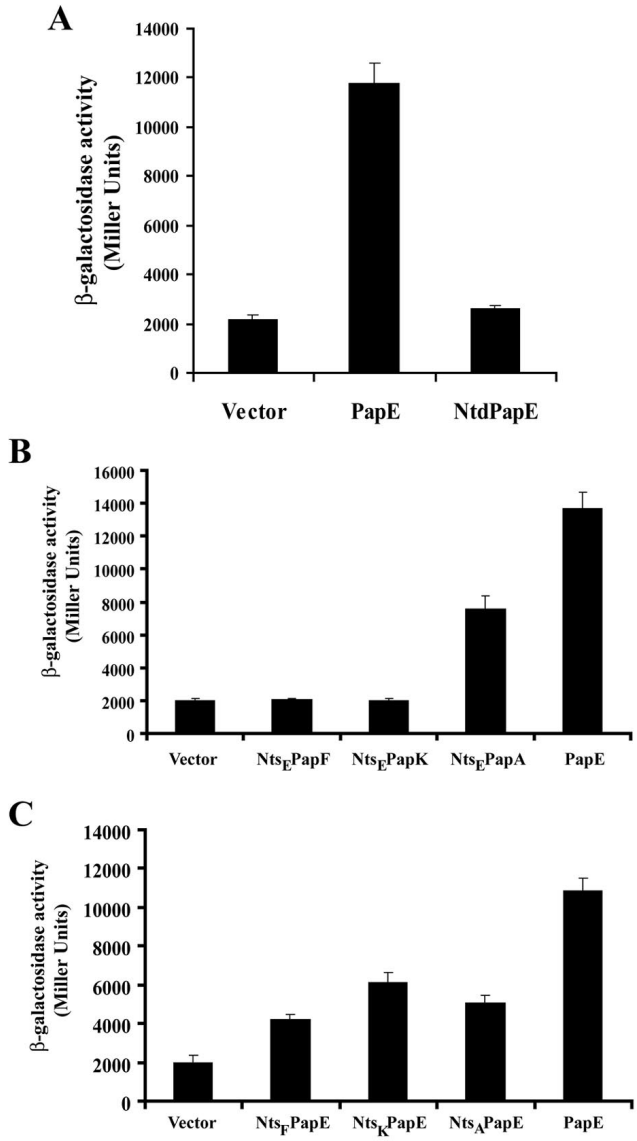

FIG. 3. Activation of the Cpx signaling pathway by PapE is dependent upon the presence of the N-terminal extension. (A) Removal of the N-terminal extension of PapE abolishes its ability to activate the Cpx pathway. The expression of a *cpxP′-lacZ*$^+$ fusion in response to wild-type PapE or NtdPapE was compared. β-Galactosidase activity levels were assayed as described for Fig. 2 for the following strains: empty vector (TR50/pMMB66), PapE (TR50/pHJ13), and NtdPapE (TR50/pYML36). The results plotted on the graph are the means and standard deviations of the results from three assays. (B) The PapE N-terminal extension is not sufficient for induction of Cpx by PapE. The expression of the *cpxP′-lacZ*$^+$ fusion in response to production of various Nts_EPapN subunits was measured. β-Galactosidase activity levels were assayed as described in the legend to Fig. 2 for the following strains: empty vector (TR50/pMMB66), Nts_EPapF (TR50/pYML55), Nts_EPapK (TR50/pYML75), Nts_EPapA (TR50/pYML80), and PapE (TR50/pHJ13). (C) An N-terminal extension is required for Cpx activation by the Ig-like fold of PapE. The expression of the *cpxP′-lacZ*$^+$ fusion in response to production of various Nts_NPapE subunits was measured. β-Galactosidase activity levels were assayed as described in the legend to Fig. 2 for the following strains: empty vector (TR50/pMMB66), Nts_FPapE (TR50/pYML56), Nts_KPapE (TR50/pYML83), Nts_APapE (TR50/pYML87), and PapE (TR50/pHJ13).

bars). Thus, the N-terminal extension of PapE was the most proficient in eliciting a Cpx response, with wild-type PapE activating the Cpx pathway ~6-fold over the vector control (Fig. 3C, fifth bar). These results demonstrate that activation of the Cpx pathway is specifically related to structural features of PapE that require both an N-terminal extension and the PapE Ig-like domain. Furthermore, while the N-terminal extensions of other subunits may substitute for that of PapE in this process, the N-terminal extension of PapE is the most highly effective in presenting PapE as a Cpx-activating signal. There are several potential explanations for these results. The N-terminal extension of PapE may influence the presentation of PapE to the Cpx pathway by enabling nonproductive aggregation of PapE in the periplasm, by altering the overall folding of PapE, or by affecting the stability of the PapE protein. Any or all of these products may be contributing factors to Cpx activation and were investigated further as described below.

Characterization of N-terminal deleted and N-terminal swapped subunits in self-association. PapE differs from the other tip fibrillum pilus subunits, PapG, PapF, and PapK, in that it is able to self-associate into a homopolymeric fiber (51, 57). The ability of the N-terminal extension of PapE to complete the Ig-like fold of a neighboring PapE protein is thought to explain the ability of PapE to assemble into a PapE homopolymer. In accordance with this hypothesis, deletion of the N-terminal extension abolishes the self-associative properties of PapE (51). Noting that PapE, but not NtdPapE, activates Cpx (Fig. 3A), and that PapE, but not NtdPapE, forms homopolymers (see below and reference 51), the ability of various N-terminal deleted and N-terminal swapped subunits to form multimeric species was tested to determine whether there exists a correlation between self-association and Cpx recognition that may be mediated by the N-terminal extension.

PapE-PapE interactions can be visualized in a simple, previously described assay based on the stability of subunit-subunit interactions at different temperatures (51, 57). Interactions between pilus subunits are dissociated in SDS (~1.5%) at 95°C. At room temperature (22°C) in SDS, these interactions are undisturbed and can be observed by SDS-PAGE followed by immunoblot analysis as a characteristic ladder pattern of multimers (see below and references 51 and 57). These analyses allow qualitative observation of the presence or absence of monomeric or multimeric subunit species from periplasmic extracts.

Periplasmic extracts of cells coproducing PapD and wild-type PapE, NtdPapE, or Nts_FPapE were characterized for self-association between subunits (Fig. 4A), using the multimerization assay described above. Though similar interactions are presumably initiated in the absence of the chaperone, coexpression with PapD was necessary in these assays to visualize any potential interactions, since pilus subunits are quickly proteolytically degraded in the absence of the chaperone. Figure 4A shows immunoblots of periplasmic extracts, with antiserum raised against P pilus tip fibrillae. Each blot can be divided into pairs of lanes (i.e., lanes 1 and 2 and lanes 3 and 4, etc.) that contain samples from the same periplasmic extracts. Lanes in each pair therefore differ only in the temperature (95 versus 22°C) at which the periplasms were incubated prior to analysis. Boiled (95°C) periplasmic extracts from cells coexpressing PapD and PapE revealed a monomeric population of PapE

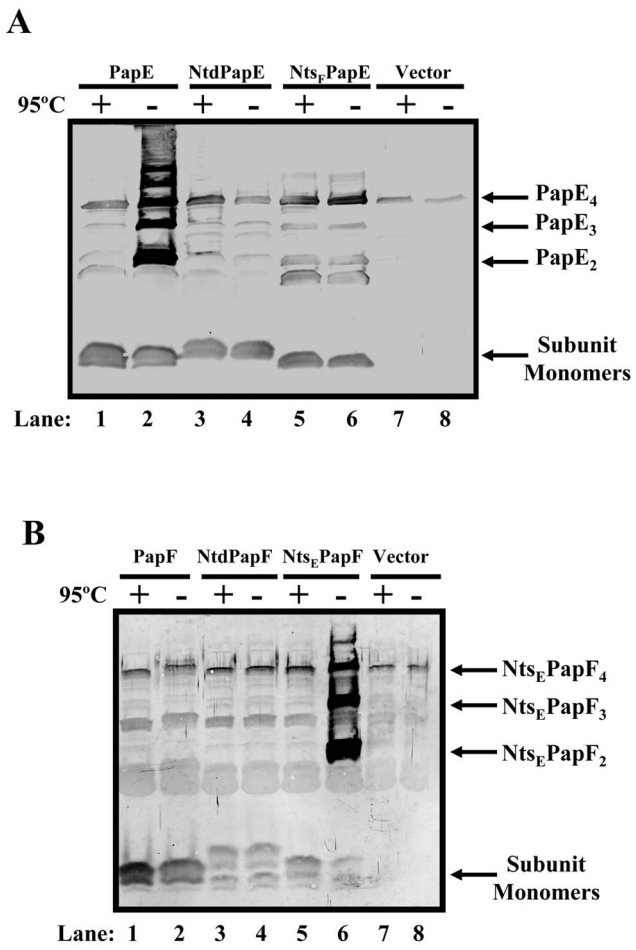

FIG. 4. Self-associative properties of wild-type, N-terminal deleted, and N-terminal swapped subunits. (A) Visualization of PapE pilus subunits from periplasmic samples that were incubated at either 95°C (+) or 22°C (−) was done by immunoblot analysis with antiserum raised against tip fibrillae. Monomeric and multimeric species are shown on the immunoblot for the following strains: lanes 1 and 2, PapD/PapE (MC4100/pWT/pHJ13); lanes 3 and 4, PapD/NtdPapE (MC4100/pWT/pYML36); lanes 5 and 6, PapD/Nts_FPapE (MC4100/pWT/pYML56); lanes 7 and 8, PapD/empty vector (MC4100/pWT/pMMB66). (B) Visualization of PapF pilus subunits from periplasmic samples that were incubated at either 95°C (+) or 22°C (−) was also done by immunoblot analysis with antiserum raised against tip fibrillae. Monomeric and multimeric species are shown on the immunoblot for the following strains: lanes 1 and 2, PapD/PapF (MC4100/pWT/pYML43); lanes 3 and 4, PapD/NtdPapF (MC4100/pWT/pYML64); lanes 5 and 6; PapD/Nts_EPapF (MC4100/pWT/pYML55); lanes 7 and 8, PapD/empty vector (MC4100/pWT/pMMB66).

subunits migrating at about 16.5 kDa (Fig. 4A, lane 1), whereas a characteristic PapE multimeric ladder ($PapE_1$, $PapE_2$, and $PapE_n$, etc.) was observed if the same periplasmic extracts were not boiled but instead incubated at 22°C prior to analysis (Fig. 4A, lane 2). The antibody preparation used in these studies was raised against polymerized Pap tips and therefore reacted more strongly with subunit oligomers than monomers. Consequently, quantitative inferences could not be made by comparing staining intensities. However, this assay provides a qualitative assessment of differences in subunit-subunit interactions as described previously (51, 57), and these differences

are striking, as shown in Fig. 4A, for example, in which the presence of higher-order multimeric species in lane 2 but not in lane 1 is plain. Periplasms from strains coexpressing PapD and NtdPapE were thus analyzed similarly. After either 95 or 22°C incubation, samples containing PapD and NtdPapE did not exhibit any multimeric complexes (Fig. 4A, lanes 3 and 4, respectively), consistent with in vitro results shown previously (51). Nts_FPapE, which has the N-terminal extension of PapF fused onto the Ig-like PapE pilin, migrated predominantly as a monomer under both 95 and 22°C conditions (Fig. 4A, lanes 5 and 6). Thus, Nts_FPapE behaved similarly to NtdPapE in self-associative properties; however, unlike NtdPapE, Nts_FPapE was able to induce a low level of Cpx activation (Fig. 3C). These results suggest that the ability of PapE to activate Cpx cannot be linked with its ability to form homopolymers. Furthermore, these results argue that the N-terminal extension of PapF does not fit into the groove of PapE, in accordance with the observed order of the subunits in the pilus fiber (Fig. 1A), and argues that the N-terminal extension not only mediates subunit-subunit interactions between PapE subunits but also determines the specificity of those interactions.

We therefore hypothesized that providing the N-terminal extension of PapE to the Ig-like domain of PapF would confer onto PapF the ability to multimerize, since the N-terminal extension of PapE is thought to fit into the groove of PapF (Fig. 1A). To test this hypothesis, we examined periplasmic extracts from cells coexpressing PapD with various forms of PapF (Fig. 4B). Although all of the various subunits could not be produced to the same levels as PapE (Fig. 4A) under the same conditions, the presence or absence of multimers were clearly detected in these assays. PapF and NtdPapF both were incapable of activating Cpx (Fig. 2A and data not shown, respectively), and both were unable to form oligomers (Fig. 4B, lanes 1 and 2 and lanes 3 and 4, respectively) at 95 and 22°C. In contrast, whereas no multimers of Nts_EPapF were detected after incubation at 95°C (Fig. 4B, lane 5), a ladder reminiscent of that seen with wild-type PapE was observed after incubation at 22°C (Fig. 4B, lane 6). Thus, the N-terminal extension of PapE allowed Nts_EPapF to interact with neighboring Nts_EPapF subunits, though it did not confer upon Nts_EPapF the ability to activate the Cpx pathway (Fig. 3B).

An alternative explanation for the ability of Nts_EPapF to multimerize is that the PapE N-terminal extension may contain unique information that directs nonspecific self-association. If this were true, then swapping the N-terminal extension of any of the subunits with that of PapE should drive them towards multimerization. Accordingly, we placed the N-terminal extension of PapE onto the Ig-like fold of PapA and PapK and tested each subunit's ability to form multimers. Neither Nts_EPapA nor Nts_EPapK was able to self-associate, even though both carried the PapE N-terminal extension (data not shown). Together, these results all demonstrate that similar to Cpx activation, PapE-PapE and PapE-PapF subunit-subunit interactions require the N-terminal extension of PapE. Furthermore, these results show that the N-terminal extension of PapE determines the binding specificity in the PapE homopolymer and in the binding to PapF, through the proper pairing of N-terminal extension and neighboring Ig-like domain.

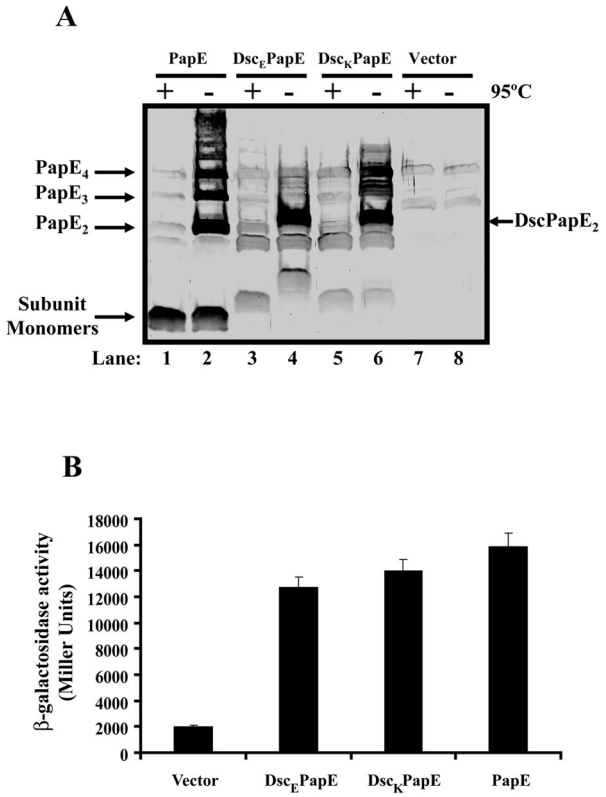

FIG. 5. Stable donor strand-complemented PapE subunits activate the Cpx pathway. (A) Monomeric and multimeric species of DscPapE pilus subunits from periplasmic samples that were incubated at either 95°C (+) or 22°C (−) were analyzed by Western blot analysis with antiserum raised against tip fibrillae. The following strains are shown in the immunoblot: lanes 1 and 2, PapD/PapE (MC4100/pWT/pHJ13); lanes 3 and 4, Dsc_EPapE (MC4100/pYML33); lanes 5 and 6, Dsc_KPapE (MC4100/pYML34); lanes 7 and 8, empty vector (MC4100/pMMB66). Note that DscPapE subunits were produced in the absence of the chaperone PapD, and each was stable in the periplasm. (B) Transcriptional activation of the *cpxP′-lacZ*$^+$ fusion was measured in β-galactosidase activity assays. β-Galactosidase activity levels were assayed as described in the legend to Fig. 2 for the following strains: vector (TR50/pMMB66), Dsc_EPapE (TR50/pYML33), Dsc_KPapE (TR50/pYML34), and PapE (TR50/pHJ13).

Stable DscPapE subunits activate Cpx. As shown above, no simple correlation could be formed between the ability of PapE to multimerize and its ability to activate the Cpx pathway. Thus, the roles of protein stability and aggregation in Cpx stimulation were next examined (Fig. 5A). Dsc_EPapE and Dsc_KPapE are stable in the periplasm without the chaperone due to the addition of either the N-terminal extension of PapE or PapK to the C terminus of PapE, which completes its Ig-like fold. In related experiments with other Dsc subunits, added donor strands also blocked interactions with other subunits by keeping the interactive groove occupied (4). To determine whether the added donor strands blocked interactions in DscPapE, these subunits were characterized in the multimerization assay (Fig. 5A). Periplasms isolated from strains carrying an empty pMMB66 vector or coexpressing wild-type PapE with PapD were also examined as controls. Dsc_EPapE was observed as a monomeric or dimeric species (Fig. 5A, lanes 3 and 4). The ability of an added donor strand to participate in

a domain swap with a neighboring subunit may explain the presence of the dimer, whereas the monomer is thought to be due to the added donor strand completing its Ig-like fold. Monomeric Dsc_EPapE exhibited a shift in apparent molecular mass when not boiled (Fig. 5A, lane 4), and while the cause of this shift is unknown, the band migrates at a molecular mass that is most consistent with it being a monomer, since the dimer was detected at a molecular mass of ~36 kDa. Interestingly, Dsc_KPapE was likewise observed in monomeric or dimeric form when incubated at room temperature prior to SDS-PAGE and immunoblotting (Fig. 5A, compare lanes 5 and 6); however, it also exhibited some ability to form trimers and higher-order multimers (Fig. 5A, lane 6).

The results presented above demonstrated that DscPapE subunits are stable in the absence of PapD and showed that each exhibited differences in self-associative properties. These subunits therefore provided an excellent means through which to further examine the role of stability and aggregation in Cpx stimulation by PapE. The expression of *cpxP'-lacZ*$^+$ was analyzed in strains expressing Dsc_EPapE or Dsc_KPapE in the absence of the PapD chaperone (Fig. 5B). Interestingly, both Dsc subunits, which exhibited different multimer-forming abilities, were capable of activating the Cpx pathway to levels comparable to those of wild-type PapE, even though both were stable in the absence of the chaperone (Fig. 5B, compare second and third bars to the fourth). Similarly, Ntd-DscPapE subunits also activated the Cpx pathway, though to a slightly lower level (~4- to 5-fold over the vector control) (data not shown). Like DscPapE subunits, each Ntd-DscPapE subunit was also stable in the periplasm in the absence of PapD, since the added donor strand completed the Ig-like fold of PapE; however, Ntd-DscPapE proteins each lacked an N-terminal extension at the amino terminus. The ability of stable DscPapE and Ntd-DscPapE subunits to activate the Cpx pathway was surprising because it was formerly thought that activation of the Cpx pathway was the result of the instability and aggregation of pilus proteins in the periplasm. These results show instead that neither aggregation nor stability are essential components of PapE-mediated activation of the Cpx pathway.

DISCUSSION

The P pilus is the prototypical member of a collection of hundreds of different adhesive organelles assembled via the chaperone-usher pathway in gram-negative organisms (references 21 and 24 and unpublished data). P pilus biogenesis involves the strict organization of multiple proteins in a tightly regulated process. In *E. coli*, assembly is monitored by the Cpx two-component signal transduction pathway (26, 28). The studies reported here take advantage of unique characteristics of PapE to begin to dissect the molecular details underlying the delicate balance between these two systems. In this work, the same region of PapE necessary for interactions between subunits during assembly was shown to also be required for PapE to be recognized by factors involved in activation of the Cpx pathway. Alterations to the topology of the pilus subunits, centered around the N-terminal extension, resulted in changes in their participation in Cpx activation, subunit-subunit interactions, and stability in the absence of the chaperone.

X-ray crystallography data from the PapD-PapK chaperone-subunit complex revealed that an 8-residue stretch at the amino terminus of PapK was disordered in the structure (50). These residues were part of an N-terminal extension present in all nonadhesin P pilus structural subunits (3, 50, 51, 56). Every pilin subunit in a pilus fiber donates its N-terminal extension to complete the Ig-like fold of its neighbor (Fig. 1A) (3, 51). These interactions were shown in the X-ray crystal structure of the complex of PapE bound to the N-terminal extension of PapK to be critical in the topological transition of the subunits into their final architecture (51). Interestingly, the G1 beta strand of the chaperone allows it to interact with all of the P pilus subunits via donor strand complementation (3, 8, 50). In contrast, alignment of the N-terminal extensions of the various structural pilus subunits revealed that each N-terminal extension is unique and varies in length (Fig. 1B). These differences among the N-terminal extensions may in part determine subunit-subunit specificity.

We found that changing the N-terminal extension of PapE to that of PapF renders Nts_FPapE incapable of self-association, whereas wild-type PapE forms multimers. We reasoned that the inability of Nts_FPapE to assemble into multimers resulted from the mispairing of the N-terminal extension of PapF with the hydrophobic groove of PapE. Consistent with this hypothesis, we were able to convert PapF into a self-associating protein simply by providing it with the PapE N-terminal extension. Multimer formation was allowed in this case because the N-terminal extension of PapE is able to complete the Ig-like fold of PapF. In contrast, swapping the N-terminal extension of PapA for that of PapE locked PapA in a monomeric state, presumably by blocking any intermolecular subunit interactions, since the incomplete Ig-like fold of PapA cannot accommodate the N-terminal extension of PapE. In support of these conclusions was the observation that Nts_EPapK also remained monomeric. These studies thus provide direct evidence that specificities of PapE-PapE and PapE-PapF interactions are the consequences of the correct pairing of the N-terminal extension and hydrophobic groove. Furthermore, in previous studies, the X-ray crystal structure of PapD-PapK showed that the Ig-like fold of PapK, like that of PapE, is also completed by the addition of a beta strand from another protein, such as a chaperone (51). Therefore, the specificity of the interactions between other structural subunits (PapG, PapK, and PapA) is likely dictated by a correct pairing of N-terminal extension to hydrophobic groove in a similar fashion to those demonstrated in these studies by PapE-PapE and PapE-PapF interactions.

We also discovered that the N-terminal extension influences the ability of PapE to activate the Cpx two-component signal transduction pathway. The Cpx pathway responds to a wide array of extracytoplasmic stresses; however, despite its varied repertoire, Cpx is still able to discriminate between similar P pilus subunits, which consist of the same overall topology. Unlike PapG and PapE, we demonstrated in this study that expression of any of the other structural subunits, PapF, PapK, and PapA, in the absence of PapD did not activate the Cpx pathway. The differential stimulation of the Cpx pathway observed in P pilus biogenesis argues that Cpx activation is a highly specific and targeted response.

Consistent with this observed specificity in Cpx activation was the finding that Cpx induction by pilin subunits could not be solely attributed to general protein processes, such as deg-

radation or stability, subunit-subunit interactions, or even levels of protein in the periplasmic compartment. DscPapE and Ntd-DscPapE subunits induced Cpx even though they are stable proteins in the absence of the chaperone. Subunit-subunit interactions, likewise, were not essential to Cpx activation. PapE and PapA are both self-associating subunits; however, these two proteins have very different N-terminal extensions and very different Cpx activation profiles. While PapE is a strong inducer of Cpx, PapA is not. Furthermore, PapF was converted into a self-associating protein by the swapping of its N-terminal extension with that of PapE, yet it was incapable of Cpx stimulation. Nts_EPapK neither self-associated nor induced Cpx. Thus, the aggregative properties of the pilins could not be correlated to Cpx activation. Finally, PapA was the most abundant subunit detectable in the periplasm in the absence of PapD, but as discussed above, it did not activate Cpx, showing that protein level did not correspond to Cpx induction or to the strength of the resultant activation. Therefore, aggregation, stability, and rate of degradation were not the most important factors in Cpx activation.

We discovered instead that simple removal of the N-terminal extension from PapE renders the resultant NtdPapE subunit incapable of Cpx activation. These results suggest that structural characteristics of the PapE pilin subunit, requiring the N-terminal extension, are responsible for its ability to activate Cpx. We showed that N-terminal extension was necessary but not sufficient to promote Cpx activation by PapE. In support of this hypothesis, neither Nts_EPapF nor Nts_EPapK activated Cpx, even though both carried the PapE N-terminal extension. Providing the N-terminal extension of PapE to the Ig-like domain of PapA enabled it to activate the Cpx pathway; however, removal of the N-terminal extension of PapA (NtdPapA) also converted PapA into a Cpx inducer. This gain of ability to activate Cpx appeared unique to PapA, as neither NtdPapF (data not shown) nor NtdPapE stimulated the Cpx pathway. Thus, Cpx induction by Nts_EPapA may result from the removal of the PapA N-terminal extension and not from the addition of the PapE N-terminal extension. Thus, while the N-terminal extension of PapE may be necessary, these results demonstrate that it is not sufficient for Cpx activation.

Accordingly, we found that the Ig-like domain of PapE was vital for Cpx activation, but it could only stimulate Cpx induction when presented in conjunction with an N-terminal extension. The N-terminal extension of PapE was the most efficient in enabling the Ig-like domain to activate the Cpx pathway; however, PapE containing any N-terminal extension swapped onto its Ig-like domain (Nts_FPapE, Nts_KPapE, and Nts_APapE) was able to activate the Cpx pathway, although to significantly lower levels than wild-type PapE. Likewise, removal of the N-terminal extension on the amino-terminal side of Dsc_EPapE and Dsc_KPapE subunits (creating Ntd-Dsc_EPapE and Ntd-Dsc_KPapE, respectively) did not severely affect the ability of the DscPapE subunits to stimulate Cpx, presumably because an N-terminal extension was still present on the carboxyl terminus. Thus, these results suggest that the Ig-like fold of PapE contributes to the Cpx-activating signal; however, an N-terminal extension is required, whether at the amino terminus or carboxyl terminus, to assist in the presentation of the OFF-pathway PapE subunit to the Cpx pathway. It is therefore possible that the N-terminal extension may play an as of yet unforeseen role in influencing the overall conformation and structure of the protein in the absence of the chaperone.

Cpx activation by PapG or PapE is abolished when each is coproduced with the chaperone PapD in the periplasm (28). The chaperone forms a stable complex with PapE via donor strand complementation, thus capping interactive surfaces on the pilin domain (51). Donor strand complementation mediated by the chaperone facilitates the folding of the subunit (3, 50, 51). Thus, the folding pathway incurred by PapE in the absence of PapD may result in an intermediate specific for Cpx activation, and the presence of the N-terminal extension may facilitate the production of this specific signal. Therefore, in the absence of the chaperone, we suspect that both the N-terminal extension and the pilin domain influence the ability of PapE to generate a signal for the Cpx pathway, possibly via a folding intermediate.

The recent three-dimensional structures of PapE in complex with PapD and in complex with a PapK N-terminal extension offered glimpses into the PapE folding pathway, demonstrating striking differences in PapE subunit structure when complexed with the different molecules (51). PapE must participate in interactions with other subunits to attain its final architecture in the pilus fiber (51); however, the molecular details of this transition are unknown. That PapE adopts a minimum of two overall architectures suggests that more conformations may also exist, during either assembly or OFF-pathway events. One or more of these may represent the signal that PapE presents to the Cpx pathway in the absence of PapD, and the N-terminal extension may assist in the formation of one of these alternate folding intermediates.

Moreover, comparisons between the crystal structures of PapD-PapK (50) and PapD-PapE (51) complexes reveal differences in structure between the subunits, such as in the locations of clusters of polar and nonpolar residues on the protein surfaces. Seemingly minute differences such as these between the overall structures may account for Cpx recognition of some subunits over others. Likewise, the PapG adhesin differs from the other subunits in that it consists of a receptor-binding domain in addition to the pilin domain. It has also been shown to activate all three partially overlapping stress response systems, σ^E, BaeSR, and CpxRA, unlike PapE (14, 28, 44). Thus, dissection of the activating signal in PapG will likely reveal further nuances not found in PapE, and stimulation of Cpx by PapG may or may not follow the same pathway. Studies are under way to begin to examine this question.

In conclusion, despite possessing the same overall topology, the work described in this study demonstrates the individuality of each of the P pilus structural subunits. Each subunit appears to have specific functions in both the pilus fiber and the biogenesis pathway. Notably, PapG and PapE are the only two subunits in the pilus found thus far that activate Cpx. Interestingly, as pili are assembled in a top-down fashion (62), PapG and PapE are also among the first subunits to be integrated into the growing pilus at the cell surface. PapG may thus report to the cell that pilus biogenesis has begun, whereas PapE can instruct the cell to continue the process. Abundant expression of PapE would ensure that enough protein is made for both incorporation into the pilus fiber and for activation of the Cpx pathway. Cpx activates transcription of protein folding factors, such as DsbA, that are necessary for P pilus biogenesis while at

the same time positively affecting *pap* expression (26). This commits the cells to producing more pili and simultaneously facilitates their assembly, which may therefore ensure that daughter cells also acquire pili and survive in the urinary tract (26). Thus, in this manner, *E. coli* can maintain tight control over the biogenesis of pili, allowing proper presentation of pili when needed. This work showed that the same surface on PapE that confers specificity between subunit-subunit interactions also plays an important role in the activation of the Cpx two-component signal transduction pathway. In this way, PapE could serve the dual function of providing flexibility in the tip fibrillum while also signaling the cell to commit to the process of pilus construction.

ACKNOWLEDGMENTS

We thank Karen W. Dodson for valuable insight and helpful discussions and for providing the *papG1* plasmid. We are also grateful to other members of the Hultgren lab for helpful discussions, especially Sheryl S. Justice for her aid in the critical review of the manuscript.

This work was supported by NIH grants AI29549 and AI48689 (to S.J.H.) and by NIGMS MERIT award GM34821 (to T.J.S.).

REFERENCES

1. **Baga, M., M. Norgren, and S. Normark.** 1987. Biogenesis of *E. coli* Pap pili: PapH, a minor pilin subunit involved in cell anchoring and length modulation. Cell **49:**241–251.
2. **Baga, M., S. Normark, J. Hardy, P. O'Hanley, D. Lark, O. Olsson, G. Schoolnik, and S. Falkow.** 1984. Nucleotide sequence of the gene encoding the *papA* pilus subunit of human uropathogenic *Escherichia coli*. J. Bacteriol. **157:**330–333.
3. **Barnhart, M. M., J. S. Pinkner, G. E. Soto, F. G. Sauer, S. Langermann, G. Waksman, C. Frieden, and S. J. Hultgren.** 2000. PapD-like chaperones provide the missing information for folding of pilin proteins. Proc. Natl. Acad. Sci. USA **97:**7709–7714.
4. **Barnhart, M. M., F. G. Sauer, J. S. Pinkner, and S. J. Hultgren.** 2003. Chaperone-subunit-usher interactions required for donor strand exchange during bacterial pilus assembly. J. Bacteriol. **185:**2723–2730.
5. **Bock, K., M. E. Breimer, A. Brignole, G. C. Hansson, K.-A. Karlsson, G. Larson, H. Leffler, B. E. Samuelsson, N. Strömberg, C. Svanborg-Edén, and J. Thurin.** 1985. Specificity of binding of a strain of uropathogenic *Escherichia coli* to Galα(1–4)Gal-containing glycosphingolipids. J. Biol. Chem. **260:**8545–8551.
6. **Bullitt, E., and L. Makowski.** 1995. Structural polymorphism of bacterial adhesion pili. Nature **373:**164–167.
7. **Casadaban, M. J.** 1976. Transposition and fusion of lac genes to selected promoters in Escherichia coli using bacteriophages lambda and Mu. J. Mol. Biol. **104:**541–555.
8. **Choudhury, D., A. Thompson, V. Sojanoff, S. Langermann, J. Pinkner, S. J. Hultgren, and S. Knight.** 1999. X-ray structure of the FimC-FimH chaperone-adhesin complex from uropathogenic *Escherichia coli*. Science **285:**1061–1065.
9. **Connolly, L., A. D. L. Penas, B. M. Alba, and C. A. Gross.** 1997. The response to extracytoplasmic stress in *Escherichia coli* is controlled by partially overlapping pathways. Genes Dev. **11:**2012–2021.
10. **Cosma, C. L., P. N. Danese, J. H. Carlson, T. J. Silhavy, and W. B. Snyder.** 1995. Mutational activation of the Cpx signal transduction pathway of *Escherichia coli* suppresses the toxicity conferred by certain envelope-associated stresses. Mol. Microbiol. **18:**491–505.
11. **Danese, P. N., and T. J. Silhavy.** 1998. CpxP, a stress-combative member of the Cpx regulon. J. Bacteriol. **180:**831–839.
12. **Danese, P. N., and T. J. Silhavy.** 1997. The σ^E and the Cpx signal transduction systems control the synthesis of periplasmic protein-folding systems in *Escherichia coli*. Genes Dev. **11:**1183–1193.
13. **De Wulf, P., A. M. McGuire, X. Liu, and E. C. C. Lin.** 2002. Genome-wide profiling of promoter recognition by the two-component response regulator CpxR-P in *Escherichia coli*. J. Biol. Chem. **277:**26652–26661.
14. **DiGiuseppe, P. A., and T. J. Silhavy.** 2003. Signal detection and target gene induction by the CpxRA two-component system. J. Bacteriol. **185:**2432–2440.
15. **Dodson, K. W., F. Jacob-Dubuisson, R. T. Striker, and S. J. Hultgren.** 1993. Outer membrane PapC usher discriminately recognizes periplasmic chaperone-pilus subunit complexes. Proc. Natl. Acad. Sci. USA **90:**3670–3674.
16. **Furste, J. P., W. Pansegrau, R. Frank, H. Blocker, P. Scholz, M. Bagdasarian, and E. Lanka.** 1986. Molecular cloning of the plasmid RP4 primase region in a multi-host-range tacP expression vector. Gene **48:**119–131.
17. **Gong, M., and L. Makowski.** 1992. Helical structure of Pap adhesion pili from *Escherichia Coli*. J. Mol. Biol. **228:**735–742.
18. **Holmgren, A., and C. Brändén.** 1989. Crystal structure of chaperone protein PapD reveals an immunoglobulin fold. Nature **342:**248–251.
19. **Holmgren, A., M. J. Kuehn, C.-I. Brändén, and S. J. Hultgren.** 1992. Conserved imunoglobulin-like features in a family of periplasmic pilus chaperones in bacteria. EMBO J. **11:**1617–1622.
20. **Hull, R. A., R. E. Gill, P. Hsu, B. H. Minshaw, and S. Falkow.** 1981. Construction and expression of recombinant plasmids encoding type 1 and D-mannose-resistant pili from a urinary tract infection *Escherichia coli* isolate. Infect. Immun. **33:**933–938.
21. **Hultgren, S. J., S. N. Abraham, M. G. Caparon, P. Falk, J. W. St. Geme III, and S. Normark.** 1993. Pilus and non-pilus bacterial adhesins: assembly and function in cell recognition. Cell **73:**887–901.
22. **Hultgren, S. J., F. Lindberg, G. Magnusson, J. Kihlberg, J. M. Tennent, and S. Normark.** 1989. The PapG adhesin of uropathogenic *Escherichia coli* contains separate regions for receptor binding and for the incorporation into the pilus. Proc. Natl. Acad. Sci. USA **86:**4357–4361.
23. **Hung, D. L., S. D. Knight, and S. J. Hultgren.** 1999. Probing conserved surfaces on PapD. Mol. Microbiol. **31:**773–783.
24. **Hung, D. L., S. D. Knight, R. M. Woods, J. S. Pinkner, and S. J. Hultgren.** 1996. Molecular basis of two subfamilies of immunoglobulin-like chaperones. EMBO J. **15:**3792–3805.
25. **Hung, D. L., J. S. Pinkner, S. D. Knight, and S. J. Hultgren.** 1999. Structural basis of chaperone self-capping in P pilus biogenesis. Proc. Natl. Acad. Sci. USA **96:**8178–8183.
26. **Hung, D. L., T. L. Raivio, C. H. Jones, T. J. Silhavy, and S. J. Hultgren.** 2001. Cpx signaling pathway monitors biogenesis and affects assembly and expression of P pili. EMBO J. **20:**1508–1518.
27. **Jacob-Dubuisson, F., J. Heuser, K. Dodson, S. Normark, and S. J. Hultgren.** 1993. Initiation of assembly and association of the structural elements of a bacterial pilus depend on two specialized tip proteins. EMBO J. **12:**837–847.
28. **Jones, C. H., P. N. Danese, J. S. Pinkner, T. J. Silhavy, and S. J. Hultgren.** 1997. The chaperone-assisted membrane release and folding pathway is sensed by two signal transduction systems. EMBO J. **16:**6394–6406.
29. **Jones, C. H., K. Dodson, and S. J. Hultgren.** 1996. Structure, function, and assembly of adhesive P pili, p. 175–219. *In* H. L. T. Mobley and J. W. Warren (ed.), Urinary tract infections: molecular pathogenesis and clinical management, 1st ed. ASM Press, Washington, D.C.
30. **Kuehn, M. J., J. Heuser, S. Normark, and S. J. Hultgren.** 1992. P pili in uropathogenic *E. coli* are composite fibres with distinct fibrillar adhesive tips. Nature **356:**252–255.
31. **Kuehn, M. J., S. Normark, and S. J. Hultgren.** 1991. Immunoglobulin-like PapD chaperone caps and uncaps interactive surfaces of nascently translocated pilus subunits. Proc. Natl. Acad. Sci. USA **88:**10586–10590.
32. **Kuehn, M. J., D. J. Ogg, J. Kihlberg, L. N. Slonim, K. Flemmer, T. Bergfors, and S. J. Hultgren.** 1993. Structural basis of pilus subunit recognition by the PapD chaperone. Science **262:**1234–1241.
33. **Leffler, H., and C. Svanborg-Eden.** 1980. Chemical identification of a glycosphingolipid receptor for *Escherichia coli* attaching to human urinary tract epithelial cells and agglutinating human erythrocytes. FEMS Microbiol. Lett. **8:**127–134.
34. **Lindberg, F., B. Lund, L. Johansson, and S. Normark.** 1987. Localization of the receptor-binding protein adhesin at the tip of the bacterial pilus. Nature **328:**84–87.
35. **Lindberg, F., J. M. Tennent, S. J. Hultgren, B. Lund, and S. Normark.** 1989. PapD, a periplasmic transport protein in P-pilus biogenesis. J. Bacteriol. **171:**6052–6058.
36. **Lindberg, F. P., B. Lund, and S. Normark.** 1984. Genes of pyelonephritogenic *E. coli* required for digalactoside-specific agglutination of human cells. EMBO J. **3:**1167–1173.
37. **Lund, B., F. Lindberg, B. I. Marklund, and S. Normark.** 1987. The PapG protein is the alpha-D-galactopyranosyl-(1–4)-beta-D-galactopyranose-binding adhesin of uropathogenic *Escherichia coli*. Proc. Natl. Acad. Sci. USA **84:**5898–5902.
38. **Mileykovskaya, E., and W. Dowhan.** 1997. The Cpx two-component signal transduction pathway is activated in *Escherichia coli* mutant strains lacking phosphatidylethanolamine. J. Bacteriol. **179:**1029–1034.
39. **Morrison, H. G., and R. C. Desrosiers.** 1993. A PCR-based strategy for extensive mutagenesis of a target DNA sequence. BioTechniques **14:**454–457.
40. **Mulvey, M. A.** 2002. Adhesion and entry of uropathogenic *Escherichia coli*. Cell. Microbiol. **4:**257–271.
41. **Mulvey, M. A., J. D. Schilling, J. J. Martinez, and S. J. Hultgren.** 2000. Bad bugs and beleaguered bladders: interplay between uropathogenic Escherichia coli and innate host defenses. Proc. Natl. Acad. Sci. USA **97:**8829–8835.
42. **Nakayama, S. I., and H. Watanabe.** 1995. Involvement of CpxA, a sensor of a two-component regulatory system, in the pH-dependent regulation of expression of Shigella sonnei *virF* gene. J. Bacteriol. **177:**5062–5069.
43. **Pogliano, J., A. S. Lynch, D. Belin, E. C. C. Lin, and J. Beckwith.** 1997. Regulation of *Escherichia coli* cell envelope proteins involved in protein

folding and degradation by the Cpx two-component system. Genes Dev. **11:**1169–1182.
44. **Raffa, R. G., and T. L. Raivio.** 2002. A third envelope stress signal transduction pathway in *Escherichia coli*. Mol. Microbiol. **45:**1599–1611.
45. **Raivio, T. L., M. W. Laird, J. C. Joly, and T. J. Silhavy.** 2000. Tethering of CpxP to the inner membrane prevents spheroplast induction of the Cpx envelope stress response. Mol. Microbiol. **37:**1186–1197.
46. **Raivio, T. L., D. L. Popkin, and T. J. Silhavy.** 1999. The Cpx envelope stress response is controlled by amplification and feedback inhibition. J. Bacteriol. **181:**5263–5272.
47. **Raivio, T. L., and T. J. Silhavy.** 1999. The σ^E and Cpx regulatory pathways: overlapping but distinct envelope stress responses. Curr. Opin. Microbiol. **2:**159–165.
48. **Raivio, T. L., and T. J. Silhavy.** 1997. Transduction of envelope stress in *Escherichia coli* by the Cpx two-component system. J. Bacteriol. **179:**7724–7733.
49. **Roberts, J. A., B.-I. Marklund, D. Ilver, D. Haslam, M. B. Kaack, G. Baskin, M. Louis, R. Mollby, J. Winberg, and S. Normark.** 1994. The Gal α(1–4) Gal-specific tip adhesin of *Escherichia coli* P-fimbriae is needed for pyelonephritis to occur in the normal urinary tract. Proc. Natl. Acad. Sci. USA **91:**11889–11893.
50. **Sauer, F. G., K. Futterer, J. S. Pinkner, K. W. Dodson, S. J. Hultgren, and G. Waksman.** 1999. Structural basis of chaperone function and pilus biogenesis. Science **285:**1058–1061.
51. **Sauer, F. G., J. S. Pinkner, G. Waksman, and S. J. Hultgren.** 2002. Chaperone priming of pilus subunits facilitates a topological transition that drives fiber formation. Cell **111:**543–551.
52. **Saulino, E. T., E. Bullitt, and S. J. Hultgren.** 2000. Snapshots of usher-mediated protein secretion and ordered pilus assembly. Proc. Natl. Acad. Sci. USA **97:**9240–9245.
53. **Saulino, E. T., D. G. Thanassi, J. Pinkner, and S. J. Hultgren.** 1998. Ramifications of kinetic partitioning on usher-mediated pilus biogenesis. EMBO J. **17:**2177–2185.
54. **Slonim, L. N., J. S. Pinkner, C. I. Branden, and S. J. Hultgren.** 1992. Interactive surface in the PapD chaperone cleft is conserved in pilus chaperone superfamily and essential in subunit recognition and assembly. EMBO J. **11:**4747–4756.
55. **Snyder, W. B., L. J. Davis, P. N. Danese, C. L. Cosma, and T. J. Silhavy.** 1995. Overproduction of NlpE, a new outer membrane lipoprotein, suppresses the toxicity of periplasmic LacZ by activation of the Cpx signal transduction pathway. J. Bacteriol. **177:**4216–4223.
56. **Soto, G. E., K. W. Dodson, D. Ogg, C. Liu, J. Heuser, S. Knight, J. Kihlberg, C. H. Jones, and S. J. Hultgren.** 1998. Periplasmic chaperone recognition motif of subunits mediates quaternary interactions in the pilus. EMBO J. **17:**6155–6167.
57. **Striker, R., F. Jacob-Dubuisson, C. Frieden, and S. J. Hultgren.** 1994. Stable fiber forming and non-fiber forming chaperone-subunit complexes in pilus biogenesis. J. Biol. Chem. **269:**12233–12239.
58. **Stromberg, N., B. I. Marklund, B. Lund, D. Ilver, A. Hamers, W. Gaastra, K. A. Karlsson, and S. Normark.** 1990. Host-specificity of uropathogenic *Escherichia coli* depends on differences in binding specificity to Galα(1–4)Gal-containing isoreceptors. EMBO J. **9:**2001–2010.
59. **Thanassi, D. G., and S. J. Hultgren.** 2000. Assembly of complex organelles: pilus biogenesis in gram-negative bacteria as a model system. Methods **20:** 111–126.
60. **Thanassi, D. G., E. T. Saulino, and S. J. Hultgren.** 1998. The chaperone/usher pathway: a major terminal branch of the general secretory pathway. Curr. Opin. Microbiol. **1:**223–231.
61. **Thanassi, D. G., E. T. Saulino, M.-J. Lombardo, R. Roth, J. Heuser, and S. J. Hultgren.** 1998. The PapC usher forms an oligomeric channel: implications for pilus biogenesis across the outer membrane. Proc. Natl. Acad. Sci. USA **95:**3146–3151.
62. **Thanassi, D. G., C. Stathopoulos, K. Dodson, D. Geiger, and S. J. Hultgren.** 2002. Bacterial outer membrane ushers contain distinct targeting and assembly domains for pilus biogenesis. J. Bacteriol. **184:**6260–6269.
63. **Wertman, K. F., A. R. Wyman, and D. Botstein.** 1986. Host/vector interactions which affect the viability of recombinant phage lambda clones. Gene **49:**253–262.